Dispersion and Asymmetry Effects of ADI-FDTD

Michael Darms, Rolf Schuhmann, Holger Spachmann, and Thomas Weiland

***Abstract*—In this paper, a generalized derivation of the alternating direction implicit finite-difference time-domain algorithm based on operator splitting is proposed. The formulation follows the notation of the finite integration technique. A straightforward proof of stability is given and the numerical dispersion formula is presented and verified by numerical experiments. As an additional parasitic effect, the *asymmetric behavior* of the algorithm even for exactly symmetric setups is revealed. Both the dispersion error and the asymmetry error are discussed in terms of the applicability of ADI for low-frequency problems.**

***Index Terms*—alternating direction implicit (ADI), finite-difference time-domain (FDTD), finite integration technique (FIT), stability.**

I. Introduction

In recent publications [1], [2] the alternating direction implicit (ADI) has been adapted to the finite-difference time-domain (FDTD) approach [3] for electromagnetic problems. Compared to the conventional leapfrog algorithm, the ADI temporal integration method offers the great advantage of being unconditionally stable, accompanied only by a small computational overhead.

So far, the accuracy of the algorithm has been analyzed by the numerical dispersion relation given in [4], [5]. Taking only the numerical dispersion into account, the ADI-FDTD algorithm should be a good choice for many problems, which can not be addressed by the conventional FDTD algorithm. However, numerical experiments [6], [7] demonstrate that there must be other sources of significant numerical errors, which limit the applicability of the ADI-FDTD method.

II. ADI-FDTD Based on Operator Splitting

A. Generalized ADI Formulation

In the following generalized description of the ADI algorithm, the matrix–vector notation of the finite integration technique (FIT [8]) is used. Applied to Cartesian grids and to time domain using the leapfrog scheme, FIT supplies computationally equivalent update formulas as the FDTD method [9].

The starting points are the discrete forms of Faraday's and Ampere's law (the first and second so-called *Maxwell's Grid Equations*)

$$\frac{d}{dt}\,\widehat{\mathbf{h}} = -\mathbf{M}_{\mu^{-1}}\mathbf{C}\,\widehat{\mathbf{e}}, \quad \frac{d}{dt}\,\widehat{\mathbf{e}} = \mathbf{M}_{\varepsilon^{-1}}\tilde{\mathbf{C}}\,\widehat{\mathbf{h}} \tag{1}$$

with the state vectors $\widehat{\mathbf{e}}$ and $\widehat{\mathbf{h}}$ (electric and magnetic grid voltages), the curl-matrices $\mathbf{C}$ and $\tilde{\mathbf{C}} = \mathbf{C}^T$ for the primary and the dual grid, and the material operators $\mathbf{M}_{\varepsilon^{-1}}$ and $\mathbf{M}_{\mu^{-1}}$ (diagonal matrices for Cartesian grids).

Based on the idea of operator splitting, the curl operator can be arbitrarily separated in $\mathbf{C} = \mathbf{C}_1 + \mathbf{C}_2$ and $\tilde{\mathbf{C}} = \tilde{\mathbf{C}}_1 + \tilde{\mathbf{C}}_2$ with $\tilde{\mathbf{C}}_1 = \mathbf{C}_1^T$ and $\tilde{\mathbf{C}}_2 = \mathbf{C}_2^T$. After replacing the time derivatives by central differences one can define two half steps of a generalized ADI-type update scheme, the *first procedure*

$$\begin{pmatrix} \mathbf{I} & -\frac{\Delta t}{2}\mathbf{M}_{\varepsilon^{-1}}\tilde{\mathbf{C}}_2 \\ \frac{\Delta t}{2}\mathbf{M}_{\mu^{-1}}\mathbf{C}_2 & \mathbf{I} \end{pmatrix} \begin{pmatrix} \widehat{\mathbf{e}}^{\,n+1/2} \\ \widehat{\mathbf{h}}^{\,n+1/2} \end{pmatrix} = \begin{pmatrix} \mathbf{I} & \frac{\Delta t}{2}\mathbf{M}_{\varepsilon^{-1}}\tilde{\mathbf{C}}_1 \\ -\frac{\Delta t}{2}\mathbf{M}_{\mu^{-1}}\mathbf{C}_1 & \mathbf{I} \end{pmatrix} \begin{pmatrix} \widehat{\mathbf{e}}^{\,n} \\ \widehat{\mathbf{h}}^{\,n} \end{pmatrix} \tag{2}$$

and the *second procedure*

$$\begin{pmatrix} \mathbf{I} & -\frac{\Delta t}{2}\mathbf{M}_{\varepsilon^{-1}}\tilde{\mathbf{C}}_1 \\ \frac{\Delta t}{2}\mathbf{M}_{\mu^{-1}}\mathbf{C}_1 & \mathbf{I} \end{pmatrix} \begin{pmatrix} \widehat{\mathbf{e}}^{\,n+1} \\ \widehat{\mathbf{h}}^{\,n+1} \end{pmatrix} = \begin{pmatrix} \mathbf{I} & \frac{\Delta t}{2}\mathbf{M}_{\varepsilon^{-1}}\tilde{\mathbf{C}}_2 \\ -\frac{\Delta t}{2}\mathbf{M}_{\mu^{-1}}\mathbf{C}_2 & \mathbf{I} \end{pmatrix} \begin{pmatrix} \widehat{\mathbf{e}}^{\,n+1/2} \\ \widehat{\mathbf{h}}^{\,n+1/2} \end{pmatrix}. \tag{3}$$

Both update equations can be symmetrized using the transformations $\widehat{\mathbf{e}}' = \mathbf{M}_{\varepsilon^{-1}}^{-1/2}\widehat{\mathbf{e}}$ and $\widehat{\mathbf{h}}' = \mathbf{M}_{\mu^{-1}}^{-1/2}\widehat{\mathbf{h}}$.

B. Stability

The resulting (symmetrized) system matrix for a full time step is a so called *Peaceman–Rachford* matrix and can be written as

$$\mathbf{G} = (\mathbf{I} - r\mathbf{Y}_1)^{-1}(\mathbf{I} + r\mathbf{Y}_2)(\mathbf{I} - r\mathbf{Y}_2)^{-1}(\mathbf{I} + r\mathbf{Y}_1) \tag{4}$$

with $r = \Delta t/2$ and the anti-symmetric matrices

$$\mathbf{Y}_n = \begin{pmatrix} 0 & \mathbf{M}_{\varepsilon^{-1}}^{1/2}\tilde{\mathbf{C}}_n\mathbf{M}_{\mu^{-1}}^{1/2} \\ -\mathbf{M}_{\mu^{-1}}^{1/2}\mathbf{C}_n\mathbf{M}_{\varepsilon^{-1}}^{1/2} & 0 \end{pmatrix}. \tag{5}$$

The matrix $\mathbf{G}$ is similar to the matrix $\mathbf{G}' = (\mathbf{I} - r\mathbf{Y}_1)\mathbf{G}(\mathbf{I} - r\mathbf{Y}_1)^{-1}$. Using the general relation $(\mathbf{I} - \mathbf{A})(\mathbf{I} + \mathbf{A})^{-1} = (\mathbf{I} + \mathbf{A})^{-1}(\mathbf{I} - \mathbf{A})$, it can be shown [6] that $\mathbf{G}'$ is a unitary matrix ($\mathbf{G}'^T = \mathbf{G}'^{-1}$). Hence, the magnitude of all eigenvalues of $\mathbf{G}'$ and $\mathbf{G}$ is equal to one *for arbitrary time steps* $\Delta t = 2r$, which guarantees unconditional stability.

It is important to note that this proof does not depend on the special separation scheme of the curl operator. Thus, (2) and (3)

Manuscript received April 2, 2002; revised June 20, 2002. The review of this letter was arranged by Associate Editor Dr. Arvind Sharma.

The authors are with Technische Universität Darmstadt, Computational Electromagnetics Laboratory (TEMF), Darmstadt, Germany (e-mail: mdarms@hrz1.hrz.tu-darmstadt.de; schuhmann@temf.tu-darmstadt.de; spachmann@temf.tu-darmstadt.de; weiland@temf.tu-darmstadt.de).

Digital Object Identifier 10.1109/LMWC.2002.805951

are a generalization of the ADI-FDTD algorithm described in [1], [2] and lead to a family of unconditionally stable algorithms.

C. Splitting of the Curl Operator

The updated equations of the first and second procedure can be carried out by first solving an implicit equation for the electric voltages $\widehat{\mathbf{e}}$, followed by an explicit update step for $\widehat{\mathbf{h}}$. The resulting implicit equation reads

$$\left(\mathbf{I}+r^2\mathbf{M}_{\varepsilon^{-1}}\tilde{\mathbf{C}}_{2/1}\mathbf{M}_{\mu^{-1}}\mathbf{C}_{2/1}\right)\widehat{\mathbf{e}}^{new} = r\mathbf{M}_{\varepsilon^{-1}}\tilde{\mathbf{C}}\,\widehat{\mathbf{h}}+\left(\mathbf{I}-r^2\mathbf{M}_{\varepsilon^{-1}}\tilde{\mathbf{C}}_{2/1}\mathbf{M}_{\mu^{-1}}\mathbf{C}_{1/2}\right)\widehat{\mathbf{e}}^{old}. \quad (6)$$

The curl operators $\mathbf{C}$ and $\tilde{\mathbf{C}}$ consist of two-banded sub-matrices $\mathbf{P}_x$, $\mathbf{P}_y$, $\mathbf{P}_z$ (or $\tilde{\mathbf{P}}_{x/y/z} = -\mathbf{P}^T_{x/y/z}$, respectively), describing the differencing scheme in each of the coordinate directions. Thus, the special choice

$$\mathbf{C}_1 = \begin{pmatrix} 0 & -\mathbf{P}_z & 0 \\ 0 & 0 & -\mathbf{P}_x \\ -\mathbf{P}_y & 0 & 0 \end{pmatrix}, \quad \mathbf{C}_2 = \begin{pmatrix} 0 & 0 & \mathbf{P}_y \\ \mathbf{P}_z & 0 & 0 \\ 0 & \mathbf{P}_x & 0 \end{pmatrix} \quad (7)$$

with

$$\tilde{\mathbf{C}}_2\mathbf{C}_2 = \begin{pmatrix} \mathbf{P}^T_z\mathbf{P}_z & 0 & 0 \\ 0 & \mathbf{P}^T_x\mathbf{P}_x & 0 \\ 0 & 0 & \mathbf{P}^T_y\mathbf{P}_y \end{pmatrix} \quad (8)$$

results in a tridiagonal system matrix, which can be efficiently inverted. This splitting approach also leads back to the original ADI-FDTD algorithm.

III. Properties of the Solution

A. Numerical Dispersion

Using a similar approach as described in [4],[1] the numerical dispersion of the algorithm has been found [6]. Starting from the first procedure (2) and considering planar waves [$\underline{\widehat{\mathbf{e}}}^{(n+1/2)} = \underline{\xi}\,\widehat{\mathbf{e}}^n$ with $\phi = \measuredangle\underline{\xi}$], the eigenvalue-problem

$$\underbrace{\mathbf{M}_{\varepsilon^{-1}}(\tilde{\mathbf{C}}_1+\underline{\xi}\tilde{\mathbf{C}}_2)\mathbf{M}_{\mu^{-1}}(\mathbf{C}_1+\underline{\xi}\mathbf{C}_2)}_{\Lambda_1^{(e)}}\,\underline{\widehat{\mathbf{e}}} = -\left(\frac{\underline{\xi}-1}{\Delta t/2}\right)^2\underline{\widehat{\mathbf{e}}} \quad (9)$$

can be identified, leading to

$$\tan^2(\phi) = \frac{Kr_x+Kr_y+Kr_z+K^2r_xr_y+K^2r_yr_z+K^2r_zr_x}{1+K^3r_xr_yr_z} \quad (10)$$

with $r_\alpha = (\sin(k_\alpha\Delta\alpha/2)/(\Delta\alpha/2))^2$, $(\alpha = x, y, z)$, $\phi = \omega(\Delta t/2)$, and $K = (\Delta t/2)^2/\mu\epsilon$. This is equivalent to the formula presented in [4], if $Kr_x + Kr_y + Kr_z + K^2r_xr_y + K^2r_yr_z + K^2r_zr_x \le 1 + K^3r_xr_yr_z$.

[1]Note that the temporal shift operator Λ in [4] corresponds to a full time step shift of the field values while $\Lambda_1^{(e)}$ performs only a half time step shift of the electric field.

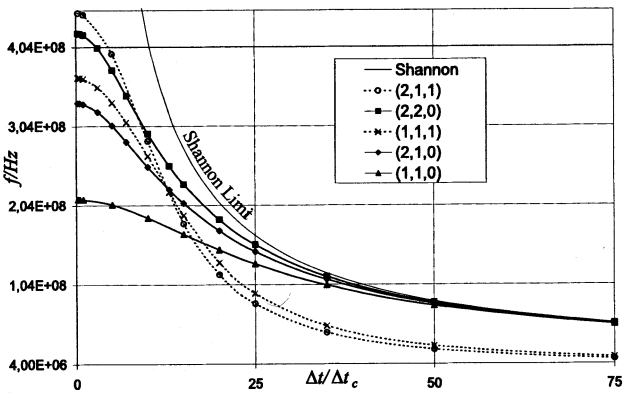

Fig. 1. Resonance frequencies of an empty cavity simulated with the ADI-FDTD algorithm for certain (n, m, k)-modes in dependence of the relative Courant number $\Delta t/\Delta t_c$. The Shannon limit indicates the highest resolvable frequency by the chosen time-step.

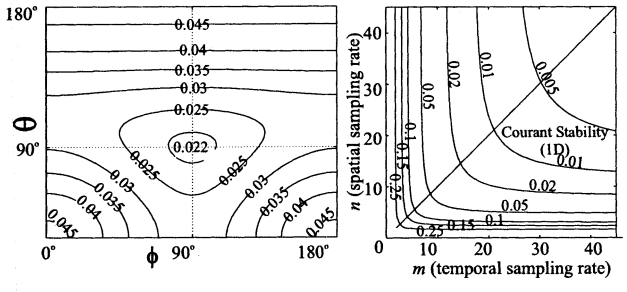

Fig. 2. Left figure shows the relative frequency error of plane waves in dependency of their incident angle in ADI-FDTD (spatial and temporal sampling rates $n = 10$ and $m = \sqrt{3}\,n$). The right figure demonstrates the relative frequency error along the axis of the grid in dependence of the spatial and temporal sampling rates $n = \lambda/\Delta$ and $m = T/\Delta t$.

To validate this dispersion relation, the resonance frequencies of several (n, m, k)-eigenmodes in a rectangular cavity (dimensions 1 m × 1 m × 0.5 m) are calculated by the ADI-algorithm followed by a fast fourier transformation (FFT), and compared to the eigensolutions predicted by (10). The spatial step size is fixed and equidistant ($\Delta x = \Delta y = \Delta z = 1/16$ m), and the time step Δt is varied within a large range, exceeding the stability range of the FDTD method (Courant-limit Δt_c).

The results of the simulations are shown in Fig. 1. For large Δt the resonance frequencies of the "two-dimensional" modes (with $k = 0$) reach the Nyquist Limit $f_{\max} = 1/(2\Delta t)$. This is also predicted by (10) as Δt tends to infinity. . In the following, the dispersion relation is used to investigate the propagation of a plane wave with $\omega = kc$ and $k_x = k\cos(\theta)\cos(\phi)$, $k_y = k\cos(\theta)\sin(\phi)$, $k_z = k\sin(\theta)$ in the grid using the ADI-FDTD scheme. The spatial and temporal sampling rates are expressed by $\Delta x = \Delta y = \Delta z = 2\pi/nk$ (equidistant grid) and $\Delta t = 2\pi/(m\omega)$. Fig. 2 (left) shows the dependency of the relative frequency error $1-\omega_{ADI}/\omega$ for $n = 10$ and $m = \sqrt{3}\,n$ (Courant limit) and varying incident angles θ and ϕ. It is evident that the maximum error arises with a propagation along the axes. Varying n and m does not change the characteristics of the plot. Fig. 2 (right) shows the frequency error of a wave propagation along the axes in dependency of the sampling rates n and m. A

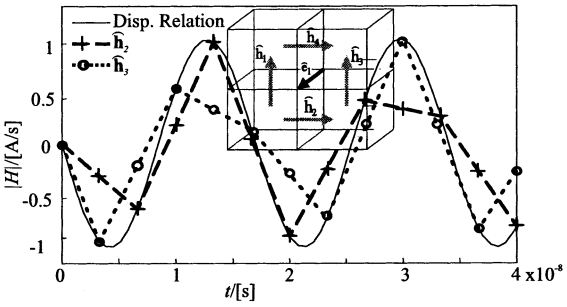

Fig. 3. Time dependency (full and half time steps) of simulated $\widehat{\mathbf{h}}_2$ and $\widehat{\mathbf{h}}_3$ component in the small cavity model with $\Delta t = 2\Delta t_c$. Alternatively, one of the components coincides with the theoretical curve, as predicted by the dispersion relation (10).

stronger impact of the error due to temporal discretization compared to the spatial can be observed. Results with only moderate frequency errors are obtained, if both the spatial and temporal sampling are sufficiently high ($n, m > 30$).

B. Symmetry

In the next section, another type of error arising in the ADI is investigated, the symmetry of its field solutions in terms of the different spatial directions in the grid. As the smallest possible numerical example, the cavity in Fig. 3 is considered. It is discretized with only four cells, PEC boundaries in all directions, and thus only one nonzero electric and four nonzero magnetic components (2-D TM-case).The spatial step size is $\Delta x = \Delta y = \Delta z = \Delta$, and the algorithm is initialized at $t = 0$ with the initial conditions $\widehat{h}_1^{(0)} = \widehat{h}_2^{(0)} = \widehat{h}_3^{(0)} = \widehat{h}_4^{(0)} = 0$, $\widehat{e}_1^{(0)} = 1$. From the symmetry of the setup, also a symmetric solution, with all $\widehat{h}_i^{(n)}$ having the same magnitude at each time step n is expected. However, substituting the initial conditions into (2) and (3) and calculating two half steps of ADI-FDTD yields

$$\eta = \frac{\widehat{h}_3^{(1)}}{\widehat{h}_4^{(1)}} = \frac{\widehat{h}_1^{(1)}}{\widehat{h}_2^{(1)}} = 1 + 2\,\frac{(\Delta t/2)^2}{\Delta^2 \mu_0 \epsilon_0} = 1 + \left(\frac{\Delta t}{2\Delta t_c}\right)^2. \quad (11)$$

Thus, there is an "asymmetry error" of the solution after one step, which grows with the Courant number $\Delta t/\Delta t_c$ squared. This effect can be explained from the operator splitting formulas (7), which introduce an artificial (nonphysical) asymmetry between the curl-operators on the grid and the dual grid. An even more surprising result can be observed, if several time steps are carried out and the time dependence of the magnetic voltage components is plotted using both *half and full time step information*. The resulting curves in Fig. 3 demonstrate that, alternatively, the component of one of the spatial directions ($\widehat{h}_2^{(1)}$ and $\widehat{h}_3^{(1)}$) coincides with the theoretical curve as predicted by the dispersion relation (10), whereas the other component is equal to the linear average of its neighboring values. There are several consequences of this peculiar behavior of the ADI algorithm: Obviously, all simulated field patterns will exhibit a parasitic asymmetry even for exactly symmetric setups. On the other side; however, this asymmetry will produce an only small effect, as long as the temporal sampling rate is sufficiently high. Thus, the poor results for low-frequency simulations with ADI cannot be fully explained by this result.

IV. Conclusion

A generalized derivation of the FDTD-ADI algorithm based on operator splitting with a compact proof of unconditional stability is proposed. The numerical dispersion relation is presented and numerically verified.

At first sight, the ADI algorithm seems to be well suited also for the low-frequency regime. However, numerical experiments show that inaccurate or even qualitatively wrong results are obtained, if the Courant-limit is considerably exceeded. As the evaluation of the numerical dispersion relation in this paper reveals, this behavior cannot be explained by the dispersion error for plane waves, since such waves are usually very well sampled in both time and space for low-frequency applications. The asymmetry error of the ADI method is also not responsible for the poor accuracy in such low-frequency cases, as it can be considered to be a small effect for well sampled waves.

In conclusion, it is evident that the investigation of plane waves is not sufficient to explain the low-frequency behavior of complex discretization approaches such as ADI. Indeed, further investigations have demonstrated that some important properties of the *eigenvectors* of the iteration matrix, including both static and dynamic solutions are hurt by the ADI method. These results and their impacts on the accuracy of the algorithm will be subject of a subsequent paper.

References

[1] T. Namiki, "3-D ADI-FDTD method—Unconditionally stable time-domain algorithm for solving full vector Maxwell's equations," *IEEE Trans. Microwave Theory Tech.*, vol. 48, pp. 1743–1748, 2000.

[2] F. Zheng, Z. Chen, and J. Zhang, "Toward the development of a three-dimensional unconditionally stable finite-difference time-domain method," *IEEE Trans. Microwave Theory Tech.*, vol. 48, pp. 1550–1558, Sept. 2000.

[3] K. Yee, "Numerical solution of initial boundary value problems involving Maxwell's equations in isotropic media," *IEEE Trans. Antennas Propagat.*, vol. 14, pp. 585–589, Mar. 1966.

[4] F. Zheng and Z. Chen, "Numerical dispersion analysis of the unconditionally stable 3-D ADI-FDTD method," *IEEE Trans. Microwave Theory Tech.*, vol. 49, pp. 1006–1009, May 2001.

[5] T. Namiki and K. Ito, "Investigation of numerical errors of the two-dimensional ADI-FDTD method," *IEEE Trans. Microwave Theory Tech.*, vol. 48, pp. 1950–2000, Nov. 2000.

[6] M. Darms, "Analyze des ADI Zeitintegrationsverfahrens für zeitlich veränderliche Feldprobleme," Darmstadt Univ. Technol., Studienarbeit, Germany, FB18, 2001.

[7] S. Garcia, T. Lee, and S. Hagness, "Accuracy limitations of the ADI-FDTD method due to truncation error," in *Proc. 18th ACES Conf.*, Monterey, CA, 2002, pp. 281–287.

[8] T. Weiland, "Eine Methode zur Lösung der Maxwellschen Gleichungen für sechskomponentige Felder auf diskreter Basis," *Arch. Elek. Übertragung.*, vol. 31, pp. 116–120, 1977.

[9] ——, "Advances in FIT/FDTD modeling," in *Proc. 18th ACES Conf.*, Monterey, CA, 2002, pp. 1-1–14.